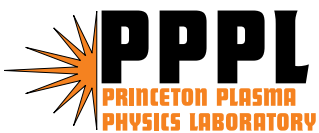


**Operation of a Segmented Hall Thruster  
with Low-sputtering Carbon-velvet Electrodes**

Y. Raitses, D. Staack,  
A. Dunaevsky, and N.J. Fisch

December 2005



# **Princeton Plasma Physics Laboratory**

## **Report Disclaimers**

---

### **Full Legal Disclaimer**

This report was prepared as an account of work sponsored by an agency of the United States Government. Neither the United States Government nor any agency thereof, nor any of their employees, nor any of their contractors, subcontractors or their employees, makes any warranty, express or implied, or assumes any legal liability or responsibility for the accuracy, completeness, or any third party's use or the results of such use of any information, apparatus, product, or process disclosed, or represents that its use would not infringe privately owned rights. Reference herein to any specific commercial product, process, or service by trade name, trademark, manufacturer, or otherwise, does not necessarily constitute or imply its endorsement, recommendation, or favoring by the United States Government or any agency thereof or its contractors or subcontractors. The views and opinions of authors expressed herein do not necessarily state or reflect those of the United States Government or any agency thereof.

### **Trademark Disclaimer**

Reference herein to any specific commercial product, process, or service by trade name, trademark, manufacturer, or otherwise, does not necessarily constitute or imply its endorsement, recommendation, or favoring by the United States Government or any agency thereof or its contractors or subcontractors.

## **PPPL Report Availability**

---

### **Princeton Plasma Physics Laboratory**

This report is posted on the U.S. Department of Energy's Princeton Plasma Physics Laboratory Publications and Reports web site in Fiscal Year 2006.

The home page for PPPL Reports and Publications is:

[http://www.pppl.gov/pub\\_report/](http://www.pppl.gov/pub_report/)

### **Office of Scientific and Technical Information (OSTI):**

Available electronically at: <http://www.osti.gov/bridge>.

Available for a processing fee to U.S. Department of Energy and its contractors, in paper from:

U.S. Department of Energy  
Office of Scientific and Technical Information  
P.O. Box 62  
Oak Ridge, TN 37831-0062

Telephone: (865) 576-8401

Fax: (865) 576-5728

E-mail: [reports@adonis.osti.gov](mailto:reports@adonis.osti.gov)

# Operation of a segmented Hall thruster with low-sputtering carbon-velvet electrodes

Y. Raitses,<sup>a)</sup> D. Staack, A. Dunaevsky and N. J. Fisch

Princeton Plasma Physics Laboratory, Princeton NJ 08543

## ABSTRACT

Carbon fiber velvet material provides exceptional sputtering resistance properties exceeding those for graphite and carbon composite materials. A 2 kW Hall thruster with segmented electrodes made of this novel material was operated in the discharge voltage range of 200-700 V. The arcing between the floating velvet electrodes and the plasma was visually observed, especially, during the initial conditioning time, which lasts for an hour. The comparison of voltage-versus current and plume characteristics of the Hall thruster with and without segmented electrodes indicates that the magnetic insulation of the segmented thruster improves with the discharge voltage at a fixed magnetic field. The observations reported here also extend the regimes wherein the segmented Hall thruster can have a narrower plume than that of the conventional non-segmented thruster.

<sup>a)</sup> Electronic mail: [yraitses@pppl.gov](mailto:yraitses@pppl.gov)

The Hall thruster<sup>1</sup> is a plasma discharge device with axial electric and radial magnetic fields applied in an annular channel. Because of the small electron mobility across the magnetic field, a substantial electric field can be maintained in quasineutral plasma. The electric field accelerates the unmagnetized ions, without dissipating much energy in the electrons. In conventional Hall thrusters (so-called stationary plasma thrusters<sup>1</sup> (SPT)), the electric field distribution is controlled mainly by the magnetic field profile along a ceramic thruster channel. However, the ion beam divergence is large, leading to erosion of the channel walls and making difficult the integration of the thruster with satellite.<sup>2-4</sup> The magnetic field curvature and electron pressure are among the factors, which can contribute to the beam divergence in Hall thrusters.<sup>3</sup> A relatively long ( $\sim 2$  cm) ion acceleration region with a large voltage drop is usually located both inside the channel and outside the channel exit, where the fringing magnetic field can lead to defocusing of the ion beam.<sup>3,4</sup>

The use of segmented electrodes along the thruster channel can provide additional control of the plasma flow in a Hall thruster.<sup>5-8</sup> The plume narrowing effect measured for molybdenum and carbon electrodes at low discharge voltages ( $\leq 300$  V)<sup>6,7</sup> was attributed to the reduced voltage drop outside the channel exit.<sup>6</sup> This effect on the voltage drop has been attributed to the lower secondary electron emission (SEE) of the electrode materials compared to that of a boron nitride ceramic and due to a shorting of the plasma electric field through the conductive electrodes.<sup>6,8</sup> Without SEE, electron energy losses at the walls are lower and contribution of electron-wall collisions to the electron-crossed field mobility (so-called near-wall conductivity<sup>1</sup>) is negligible.<sup>9-11</sup> For a constant discharge voltage, the accelerating voltage drop inside the

channel with segmented electrodes is increased,<sup>6</sup> which may lead to erosion of the electrodes due to ion-induced sputtering. In addition, ion-induced sputtering of the electrodes causes the backflow of contamination, which produces a conductive coating on the ceramic part of the thruster channel.<sup>6,7</sup> Such a coating can significantly alter the thruster operation, including an increase of the discharge current and instability of the discharge, leading to a degradation of thruster performance.<sup>6</sup> Appropriate electrode materials with a low sputtering yield are therefore important, especially for high specific impulse ( $I_{sp} \equiv v_{jet}/g$ , where  $v_{jet}$  is the jet velocity) applications,<sup>12</sup> which require a high discharge voltage operation of the Hall thruster.

**In this work** we investigate the operation of a Hall thruster with segmented electrodes made from carbon fiber velvet bonded on carbon substrates.<sup>13</sup> Sputter-resistant properties of this novel material are exceptional, particularly, with respect to the backflow of contamination.<sup>13,14</sup> This is because ions strike the velvet at grazing incidence and because sputtered particles are trapped in the velvet texture.<sup>13</sup> The total sputtering yield of carbon fiber velvet was shown to be several times lower than for carbon-carbon composite materials and graphite.<sup>14</sup> However, the low density of the velvet material may cause it to wear out faster than a denser carbon-carbon composite surface and a high-density graphite surface.<sup>14</sup> Another important feature of carbon velvet is that because of inter-fiber cavities with a large aspect ratio of  $\sim 10^2$ - $10^3$ , it is expected to suppress both ion-induced and electron-induced SEE from the electrode.<sup>15</sup> At the same time, the electric field enhancement at a fiber tip may induce the electron field emission,<sup>16,17</sup> which can, in principle, affect the plasma-wall interaction in a similar manner as the SEE.

Previous studies reported the use of a similar carbon fiber velvet material for short pulse cathodes of high power microwave tubes,<sup>16</sup> for the SEE reduction from plasma plume probes,<sup>15</sup> and for the protection of vacuum chamber walls against sputtering<sup>13</sup> in plasma thruster facilities. Here, we discuss durability of the velvet electrodes in a continuous plasma discharge of a Hall thruster and compare the discharge and plume characteristics for segmented and non-segmented thruster configurations.

A 2 kW Hall thruster (Fig 1) was operated in a 28 m<sup>3</sup> vacuum vessel equipped with cryogenic pumps. The thruster, facility and diagnostics used in these experiments are described elsewhere.<sup>18</sup> The thruster channel is made of a grade HP boron nitride ceramic. For the segmented thruster configuration, two velvet electrodes with length of 4 mm and 6 mm (Figs. 1 and 2) are placed on the inner and outer channel walls, respectively. Carbon fibers have a diameter of  $\sim 5 \times 10^{-3}$  mm and a length of  $\sim 1.5$  mm.<sup>13,14</sup> The separation distance between fibers is roughly 0.02 mm.<sup>14</sup> For the non-segmented thruster configuration, the velvet electrodes are substituted with the boron nitride spacers. In each configuration, the thruster was operated at a constant xenon mass flow rate of about 2 mg/s. The background pressure did not exceed 6  $\mu$ torr. The magnetic field (Fig. 1) was the same for all operating regimes and thruster configurations.

In the experiments described here, the measured quantities are limited to the discharge current and voltage, ion flux from the thruster, and floating potentials of the electrodes with respect to ground. The total ion flux from the thruster is obtained by integrating over the measured ion flux angular distribution. The ion flux is measured

with a guarding sleeve electrostatic probe<sup>18</sup> at the distance of 730 mm from the thruster. The probe rotates around the center of the thruster exit plane. From the ion flux and discharge current measurements we deduced the current utilization,  $I_i/I_d$ , which characterizes how effectively the magnetic field impedes the electron crossed-field current.<sup>1,11,19</sup> The plume angle was estimated for 90% of the total ion flux in a similar manner as described in Ref. 6. The standard deviation of the ion flux and plume angle measurements is generally less than  $\pm 2.5$  %.

For the segmented thruster, the measurements were carried out in the discharge voltage range of 200-700 V. The electrodes were floating. The total operation time in these regimes was roughly 50 hours. Post-run inspection of the thruster revealed no presence of a low resistance coating on ceramic walls of the thruster channel. During the thruster operation we encountered arcing between the velvet electrodes and the plasma. The arcing was quite frequent at the beginning of the thruster operation (~1 hour), but then it ceased almost completely, except for a rare occurrence at discharge voltages above 500 V. From a microscope analysis of the velvet electrodes, we found that a time-dependent cessation of the arcing correlates in time with the removal of protrusive fibers from the velvet surface. This observation suggests that the arcing is probably initiated by field emission from individual fibers and micro-protrusions on fiber surfaces.

We now consider a possible mechanism of the arcing from floating electrodes. Because of large axial gradients in the thruster plasma, the sheath voltage drop,  $V_0$ , between the plasma and equipotential electrode surface increases towards the anode.<sup>8,9,20</sup> For high discharge voltage regimes (>400 V), floating potentials of the

segmented electrodes relative to the cathode are approximately equal to zero. Therefore, we can expect that the sheath voltage on the anode side of each electrode drop is comparable with the discharge voltage. Assuming a steady state sheath, we can exploit Child's law<sup>21</sup> to obtain the sheath thickness,  $s$ , and the electric field,  $E = 4/3(V_0/s)$ , at the electrode. For a typical Hall thruster operated at the discharge voltage of 200-700 V, the plasma density is  $10^{11}$ - $10^{12}$  cm<sup>-3</sup> and the electron temperature is 20-60 eV. Under such conditions, the sheath thickness for the segmented electrode is expected to be 0.1-1 mm. For a protrusion with a radius  $r$  and a length  $l$ , the electric field enhancement,<sup>22</sup>  $\beta \approx l/r$ , reaches its maximum in the sheath when  $l \approx s$ . Then, the maximum possible electric field at the protrusion,  $E_m \approx \beta E$ , is scaled as  $E_m \propto V_0 / r$ . According to the Fowler-Nordheim law,<sup>23</sup> the field strength of  $E > 10^3$  kV/mm is required to produce an appreciable field emission current. Thus, for field emission at  $V_0 \sim 200$ -700 V, micro-protrusions have to be less than  $10^{-3}$  mm in diameter, that is not unreasonable for the fiber velvet material used for the segmented electrodes.

The electron emission from the segmented electrodes can significantly change the global current balance, which governs the floating condition for each electrode. Because of the axial sheath variation, the uniformity of the floating potential is maintained by a short-circuit current through the electrode.<sup>8,9</sup> In the absence of the electron emission from the electrode, the maximum short-circuit current is limited by the ion current to the electrode.<sup>8,9</sup> With the electron emission, the short-circuit current can increase above the ion saturation current until the sheath voltage drop is large enough to sustain field emission and provided that the global floating condition is satisfied. In experiments with a smaller size (9 cm diameter) 1 kW segmented Hall



thruster,<sup>7</sup> the current measured in an electrical circuit of a cathode-biased emissive electrode (thermionic emitter made of a dispenser tungsten) was an order magnitude larger than that for a cathode-biased non-emissive electrode (~ 50 mA).

For the carbon velvet electrodes, the current through high resistance fibers is accompanied with the Joule heating.<sup>17,24</sup> In addition to ion-induced sputtering of the protrusive fibers, excessive heating of these fibers may eventually lead to a destruction of centers of field enhancement.<sup>24</sup> This may explain the arcing disappearance after the initial conditioning time of the thruster operation. Among possible current-driven distraction mechanisms are evaporation of micro-protrusions and entire protrusive fibers.<sup>24</sup> It is also possible that protrusive fibers with non-uniform electrical resistance along the current path (e.g. fibers with non-uniform cross-sectional area or at locations where the fibers are bonded to the substrate) can be lost from the electrode due to a stronger Joule heating at higher resistance points.

Fig. 3 compares the voltage versus current (V-I) characteristics measured for the segmented and non-segmented thruster configurations. The operation of the non-segmented thruster at high discharge voltages exhibits a long (up to an hour) transitional regime, which precedes a steady state operation.<sup>12,18</sup> During the transitional operation, the discharge current is always larger than the steady state value. It is actually not clear either the transitional regime is associated with a time required for the thruster to reach a thermal steady state<sup>12</sup> or one of these operating regimes is affected by sputtering effects in laboratory environments.<sup>18</sup> Similar operating regimes<sup>12</sup> and V-I characteristics<sup>9</sup> were also reported for the state-of-the-art Hall thrusters. A strong SEE from ceramic channel walls was suggested as an

explanation of the V-I characteristics at high discharge voltages.<sup>9</sup> There is a disagreement between the theory<sup>9</sup> and the experiment<sup>18</sup> with respect to the SEE effects on the electron temperature. Without going into details of this disagreement, we note that, for the transitional regime, it is indeed the increase of the electron current that leads to the increase of the discharge current and causes a degradation of the current utilization. In the steady state operation, the reduction of the current utilization above 300 V is insignificant.

Interestingly, for the segmented thruster, there is no transitional regime. Even during the conditioning time, the discharge current changes from its steady state value only for a short time, when the arcing occurs. The discharge current does not grow with the discharge voltage. Above 400 V, the current utilization increases to about 0.8 that is almost 40-50% and 10-15 % higher than that of the non-segmented thruster in the transitional and steady state regimes, respectively. In addition, for the segmented thruster operation above 200 V the ion flux is roughly constant, ~ 85% of the neutral gas flow. The shortening of the plasma electric field through the conductive wall is predicted to increase the discharge current in the segmented thruster, as compared with the conventional thruster.<sup>8,9</sup> The fact that this effect is not so evident from our experiments is, probably, due to the relatively small surface area of the segmented electrodes.<sup>9</sup> Finally, Fig. 4 demonstrates that the segmented thruster with the carbon velvet electrodes produces a narrower plasma plume than the conventional thruster. This result is qualitatively similar to the previous reported measurements<sup>6,7</sup> for a smaller 1 kW Hall thruster with molybdenum and graphite segmented electrodes.

We now discuss the results of the experiments using the model of a quasineutral plasma flow<sup>11</sup> in the acceleration region and referring to recent measurements of the plasma properties in the non-segmented thruster.<sup>18</sup> Neglecting the pressure gradient in Ohm's law and assuming that the average electric field is  $E = V_d/L$ , we obtain the ratio of the electron cross-field current to the ion current:

$$J_e / J_i \sim \langle \mu_{\perp} \rangle \sqrt{V_d} / L, \quad (1)$$

where  $\mu_{\perp}$  is the electron cross-field mobility,  $V_d$  is the discharge voltage,  $L$  is the length of the acceleration region, and  $\langle \rangle$  means averaging along the acceleration region. For the non-segmented thruster operating at high discharge voltages, the average electron mobility changes insignificantly in the steady state regime, but increases in the transitional regime.<sup>18</sup> In the latter case, the length of the acceleration region increases slightly with the discharge voltage. Therefore, for the transitional regime, the overall effect of the discharge voltage is the reduction of the current utilization.

For the segmented thruster, the current ratio  $J_e/J_i$  decreases with the discharge voltage. Note that in keeping with our previous studies<sup>6</sup> the plasma plume narrowing effect of the segmented electrodes is likely associated with an increase of the electric field inside the channel leading to a reduction of the ion residence time in the acceleration region and thereby, possibly, reducing defocusing effect of radial pressure gradients and magnetic field curvature on ion trajectories.<sup>3</sup> If the electric field

increases equal to or faster than  $\sqrt{V_d}$ , then it is a reduction of the electron mobility at high discharge voltages that can explain the measured V-I characteristic of this thruster. Plasma measurements are necessary for more consistent analysis of the electron mobility, which cannot be predicted by the existing Hall thruster models. Such measurements will be reported in a separate paper.

In conclusion, we demonstrated the use of low-sputtering and low-SEE carbon velvet material in the continuous plasma discharge of a Hall thruster. A certain conditioning procedure of the carbon velvet material is required in order to prevent the arcing between the electrodes and the plasma. It is particularly interesting that the magnetic insulation properties of the thruster discharge with segmented electrodes tend to improve with the discharge voltage. Note that for the state-of-the-art Hall thrusters, a typical operating procedure requires an increase of the magnetic field with the discharge voltage in order to suppress the increase of the electron current.<sup>12</sup> Theoretical models predict the need for this procedure in order to maximize the thruster performance.<sup>11,25</sup> Apparently, for the segmented thruster this is no longer a requirement. The plume narrowing effect of the carbon velvet electrodes is qualitatively consistent with the previously reported results<sup>6,7</sup> obtained for a 1 kW Hall thruster with low SEE carbon and molybdenum segmented electrodes.

## ACKNOWLEDGMENT

The authors wish to thank Prof. John D. Williams and Dr. Timothy Knowles for providing the data and helpful discussions on carbon velvet material. The authors

benefited from discussions with Mr. Artem Smirnov, Dr. Leonid Dorf, Prof. Michael Keidar and Prof. Amnon Fruchtman. This work was supported by US DOE Contract No. AC02-76CH0-3073.

## REFERENCES

1. A. I. Morozov and V. V. Savel'ev, in *Reviews of Plasma Physics*, edited by B. B. Kadomtsev and V. D. Shafranov, ( Consultants Bureau, New York, 2000), Vol. 21.
2. I. Katz, G. Jongeward, V. Davis, M. Mandell, I. Mikeladis, R. Dresseler, I. Boyd, K. Kannenberg, J. Polard and D. Kind *Proceedings of the 37<sup>th</sup> Joint Propulsion Conference and Exhibit, July, 2001, Salt-Lake City, UT* (American Institute of Aeronautics and Astronautics, Reston, VA 2001), AIAA paper No. 2001-3355.
3. A. Fruchtman and A. Cohen-Zur, *Proceedings of the 40<sup>th</sup> Joint Propulsion Conference and Exhibit, July, 2004, Fort Lauderdale, FL* (American Institute of Aeronautics and Astronautics, Reston, VA 2004), AIAA paper No. 2004-3957.
4. L. Garrigues G. J. M. Hagelaar, J. Bereilles, C. Boniface and J.-P. Boeuf, *Phys. Plasmas* **10**, 4886 (2003).
5. A. Fruchtman, N. J. Fisch and Y. Raitses, *Phys. Plasmas*, **8**, 1048 (2001).
6. Y. Raitses, L. A. Dorf, A. A. Litvak and N. J. Fisch, *J. Appl. Phys.* **88**, 1263 (2000);  
Y. Raitses, M. Keidar, D. Staack and N.J. Fisch, *J. Appl. Phys.*, **92** 4906 (2002).
7. K. Diamant, J. Pollard, R. Cohen, Y. Raitses and N. J. Fisch, *Proceedings of the 40<sup>th</sup> Joint Propulsion Conference, July 2004, Fort Lauderdale, FL* (American Institute of Aeronautics and Astronautics, Reston, VA 2004), AIAA paper No. 2004-4098.
8. D. Staack, Y. Raitses and N. J. Fisch, *Proceedings of the 28<sup>th</sup> International Electric Propulsion Conference*, March 2003, Toulouse, France (Electric Rocket Propulsion Society, Cleveland, OH 2003), IEPC paper 2003-157.

9. S. Barral, K. Makowski, Z. Peradzynski, N. Gascon and M. Dudeck, *Phys. Plasmas* **10**, 4137 (2003).
10. M. Keidar, I. Boyd and I. I. Beilis, *Phys. Plasmas* **8**, 5315 (2001).
11. E. Ahedo and D. Escobar, *J. Appl. Phys.* **96**, 983 (2004).
12. R. R. Hofer, Ph. D Thesis, University of Michigan, 2004
13. The segmented electrodes were manufacture by Energy Science Laboratories, Inc. (www.esli.com), San Diego, CA.
14. T. Knowles (Private communications 2004, 2005); J. D. Williams (Private communication, 2005).
15. S. F. Engleman and J. M. Fife, *Proceedings of the 38<sup>th</sup> Joint Propulsion Conference and Exhibit, July, 2002, Indianapolis, IN* (American Institute of Aeronautics and Astronautics, Reston, VA 2002), AIAA paper No. 2002-4255.
16. D. Shiffler, M. Ruebush, M. Haworth, R. Umstattd, M. LaCour, K. Golby, D. Zagar and T. Knowles *Rev. Sci. Instrum.* **73**, 4358 (2002).
17. A. Dunaevsky, Ya. E. Krasik, A. Krokhmal, J. Felsteiner, A. V. Gunin, I. V. Pegel and S. D. Korovin, *Proceedings of the 13<sup>th</sup> Int. Conf. On High-Power Particle Beams*, Nagaoka, Japan, June 25-30, 2000, p. 516-519; *J. Appl. Phys.* **89** 2379 (2001).
18. Y. Raitses, D. Staack, M. Keidar, N. J. Fisch, *Phys. Plasmas* **12**, 057104 (2005); Y. Raitses, D. Staack, A. Smirnov, N. J. Fisch, **12**, 073507 (2005).
19. A. Smirnov, Y. Raitses and N. J. Fisch, *Phys. Plasmas* **11**, 4922 (2004).
20. M. Keidar, I. D. Boyd and I. Beilis, *Phys. Plasmas*, **11**, 1715 (2004).
21. C. D. Child, *Phys. Rev.* **32**, 492 (1911).
22. G. S. Kokkorakis, A. Modinos and J. P. Xanthakis, *J. Appl. Phys.* **91**, 4580 (2001).

23. R. F. Fowler and L. W. Nordheim, Proc. R. Soc. London, Ser. A 121, 626 (1928).
24. G. A. Mesyats, in *Pulsed Power*, (Kluwer Academic/Plenum Publishers, New York, 2005) p. 32.
25. A. Cohen-Zur, A. Fruchtman, J. Askenazy and A. Gany, Phys. Plasmas 9, 4363 (2002).



## List of Figures

Figure 1. Schematic of the thruster channel of a 2kW segmented Hall thruster with superimposed magnetic field lines. The magnetic field distribution was simulated for the experimental conditions. A 4 mm long inner and 6 mm long outer segmented electrodes are made of a carbon velvet material.

Figure 2. The outer segmented electrode made of the novel material-carbon fiber velvet bonded on a carbon substrate- before (a) and after (b) thruster operation. Typical dimensions of carbon fibers are  $\sim 5 \cdot 10^{-3}$  mm diameter,  $\sim 1.5$  mm length and 0.02 mm separation distance between the neighboring fibers. The length of protrusive fibers can be up to 5 mm (top figure).

Figure 3. The voltage versus current (V-I) characteristics for the two configurations of the 2 kW Hall thruster, segmented and non-segmented. For the non-segmented thruster, the V-I characteristics were measured in the transitional and steady state regimes. For the segmented thruster, multiple data points are due to the irreproducibility of the discharge current after variations of the discharge voltage.

Figure 4. The plume narrowing effect of the segmented electrodes. A comparison of half plume angle estimated for 90% of the total ion flux measured for the non-segmented thruster in a steady state regime and for the segmented thruster with velvet electrodes. The standard deviation of the plume measurements is less than  $\pm 3\%$ .

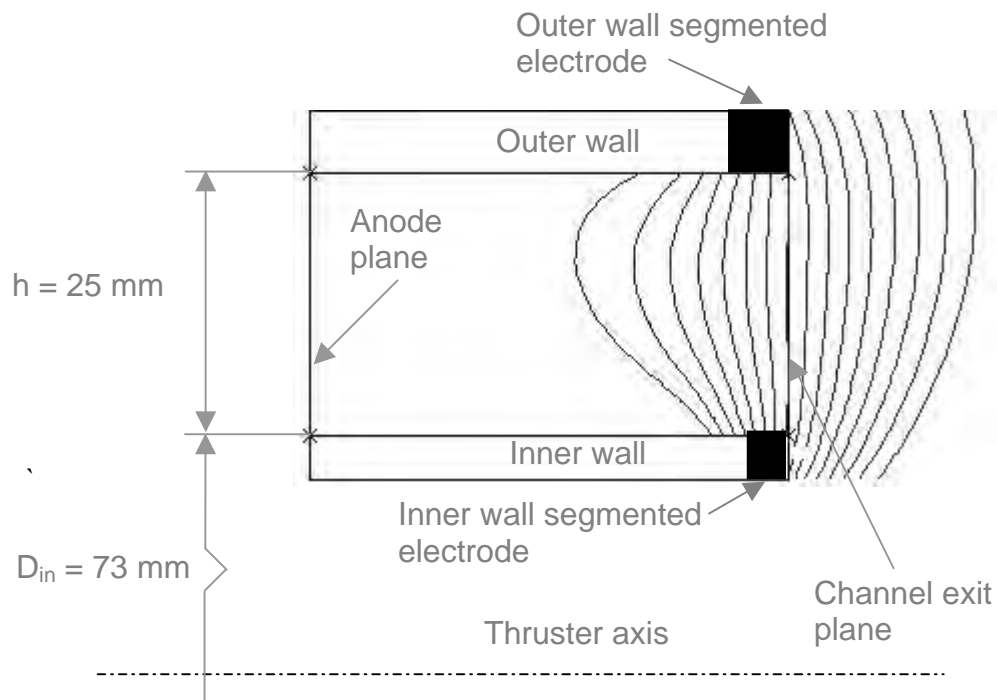
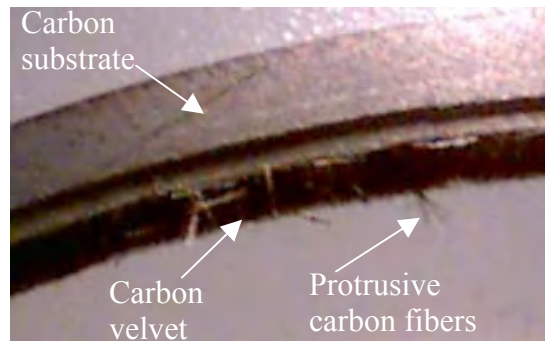


Figure 1. Schematic of the thruster channel of a 2kW segmented Hall thruster with superimposed magnetic field lines. The magnetic field distribution was simulated for the experimental conditions. A 4 mm long inner and 6 mm long outer segmented electrodes are made of a carbon velvet material.

(a)



(b)

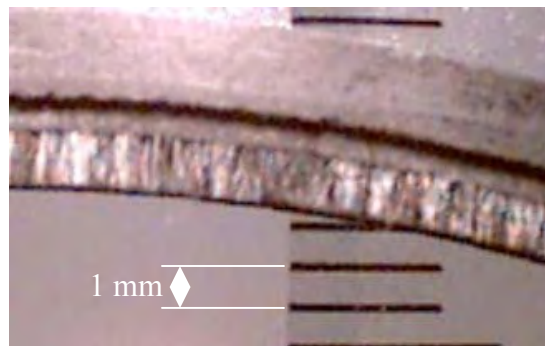


Figure 2. The outer segmented electrode made of the novel material- carbon fiber velvet bonded on a carbon substrate- before (a) and after (b) thruster operation. Typical dimensions of carbon fibers are  $\sim 5 \cdot 10^{-3}$  mm diameter,  $\sim 1.5$  mm length and 0.02 mm separation distance between the neighboring fibers. The length of protrusive fibers can be up to 5 mm (top figure).

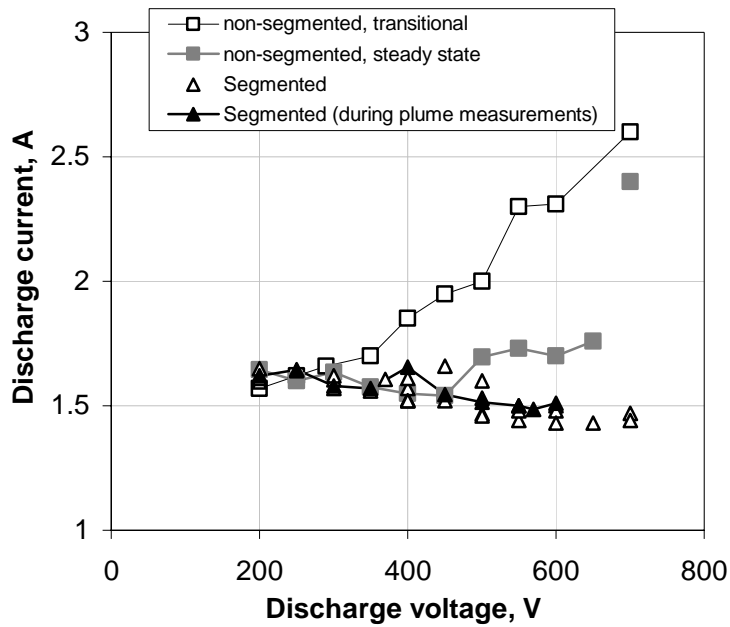


Figure 3. The voltage versus current (V-I) characteristics for the two configurations of the 2 kW Hall thruster, segmented and non-segmented. For the non-segmented thruster, the V-I characteristics were measured in the transitional and steady state regimes. For the segmented thruster, multiple data points are due to the irreproducibility of the discharge current after variations of the discharge voltage.

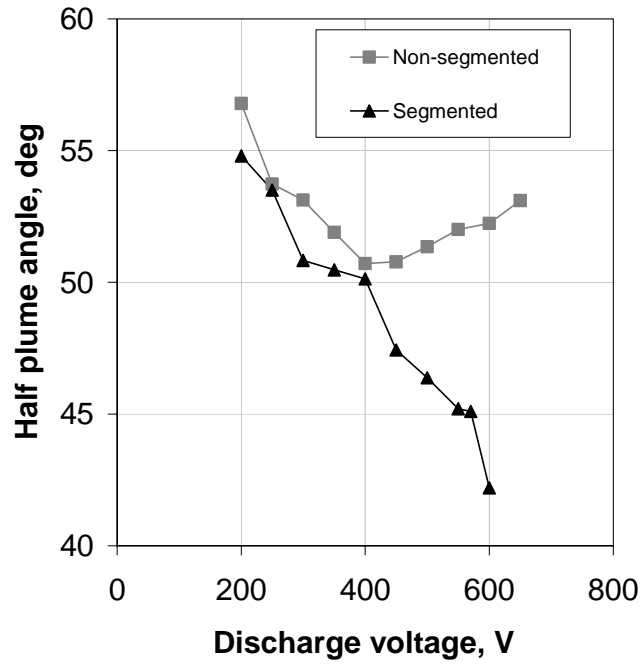


Figure 4. The plume narrowing effect of the segmented electrodes. A comparison of half plume angle estimated for 90% of the total ion flux measured for the non-segmented thruster in a steady state regime and for the segmented thruster with velvet electrodes. The standard deviation of the plume measurements is less than  $\pm 3\%$ .



## External Distribution

Plasma Research Laboratory, Australian National University, Australia  
Professor I.R. Jones, Flinders University, Australia  
Professor João Canalle, Instituto de Fisica DEQ/IF - UERJ, Brazil  
Mr. Gerson O. Ludwig, Instituto Nacional de Pesquisas, Brazil  
Dr. P.H. Sakanaka, Instituto Fisica, Brazil  
The Librarian, Culham Science Center, England  
Mrs. S.A. Hutchinson, JET Library, England  
Professor M.N. Bussac, Ecole Polytechnique, France  
Librarian, Max-Planck-Institut für Plasmaphysik, Germany  
Jolan Moldvai, Reports Library, Hungarian Academy of Sciences, Central Research  
Institute for Physics, Hungary  
Dr. P. Kaw, Institute for Plasma Research, India  
Ms. P.J. Pathak, Librarian, Institute for Plasma Research, India  
Dr. Pandji Triadyaksa, Fakultas MIPA Universitas Diponegoro, Indonesia  
Professor Sami Cuperman, Plasma Physics Group, Tel Aviv University, Israel  
Ms. Clelia De Palo, Associazione EURATOM-ENEA, Italy  
Dr. G. Grosso, Istituto di Fisica del Plasma, Italy  
Librarian, Naka Fusion Research Establishment, JAERI, Japan  
Library, Laboratory for Complex Energy Processes, Institute for Advanced Study,  
Kyoto University, Japan  
Research Information Center, National Institute for Fusion Science, Japan  
Professor Toshitaka Idehara, Director, Research Center for Development of Far-Infrared Region,  
Fukui University, Japan  
Dr. O. Mitarai, Kyushu Tokai University, Japan  
Mr. Adefila Olumide, Ilorin, Kwara State, Nigeria  
Dr. Jiangang Li, Institute of Plasma Physics, Chinese Academy of Sciences, People's Republic of China  
Professor Yuping Huo, School of Physical Science and Technology, People's Republic of China  
Library, Academia Sinica, Institute of Plasma Physics, People's Republic of China  
Librarian, Institute of Physics, Chinese Academy of Sciences, People's Republic of China  
Dr. S. Mirnov, TRINITI, Troitsk, Russian Federation, Russia  
Dr. V.S. Strelkov, Kurchatov Institute, Russian Federation, Russia  
Kazi Firoz, UPJS, Kosice, Slovakia  
Professor Peter Lukac, Katedra Fyziky Plazmy MFF UK, Mlynska dolina F-2, Komenskeho Univerzita,  
SK-842 15 Bratislava, Slovakia  
Dr. G.S. Lee, Korea Basic Science Institute, South Korea  
Dr. Rasulkhozha S. Sharafiddinov, Theoretical Physics Division, Institute of Nuclear Physics, Uzbekistan  
Institute for Plasma Research, University of Maryland, USA  
Librarian, Fusion Energy Division, Oak Ridge National Laboratory, USA  
Librarian, Institute of Fusion Studies, University of Texas, USA  
Librarian, Magnetic Fusion Program, Lawrence Livermore National Laboratory, USA  
Library, General Atomics, USA  
Plasma Physics Group, Fusion Energy Research Program, University of California at San Diego, USA  
Plasma Physics Library, Columbia University, USA  
Alkesh Punjabi, Center for Fusion Research and Training, Hampton University, USA  
Dr. W.M. Stacey, Fusion Research Center, Georgia Institute of Technology, USA  
Director, Research Division, OFES, Washington, D.C. 20585-1290

The Princeton Plasma Physics Laboratory is operated  
by Princeton University under contract  
with the U.S. Department of Energy.

Information Services  
Princeton Plasma Physics Laboratory  
P.O. Box 451  
Princeton, NJ 08543

Phone: 609-243-2750  
Fax: 609-243-2751  
e-mail: [pppl\\_info@pppl.gov](mailto:pppl_info@pppl.gov)  
Internet Address: <http://www.pppl.gov>